

YIELD STRESS MASTER CURVES FOR VARIOUS POLYMERS

N65 32162

BELOW THEIR GLASS TRANSITION TEMPERATURES

Jerome J. Lohr  
National Aeronautics and Space Administration  
Ames Research Center  
Moffett Field, Calif.

SYNOPSIS

3/p

Yield stress master curves are presented for poly(methyl methacrylate), polystyrene, polyvinyl chloride, and polyethylene terephthalate. Tensile yield stress was measured at strain rates varying from 0.003 in./in./min to 300 in./in./min and at temperatures varying from approximately 15° C above the glass transition temperature,  $T_g$ , to at least 100° C below  $T_g$ . The resultant yield - or in the brittle temperature range - failure stress, when plotted as a function of logarithm of strain rate, has been shifted laterally to construct a yield stress master curve similar in concept to the well-known stress relaxation master curve. These master curves cover from 12 to 18 decades of shifted strain rate. The master curve for each material has a characteristic slope which leads, in each case, to a simple equation relating yield stress to strain rate and temperature and is applicable for temperatures from  $T_g$  to approximately 100° C below  $T_g$ . The temperature-dependent shift factors,  $a_T$ , of each material were determined for both yield stress and stress relaxation over the temperature range. Comparison of these  $a_T$  curves shows that in both the ductile and brittle temperature ranges of each material, the shape of the yield stress and stress relaxation  $a_T$  curves are very similar. However, the absolute magnitude of the change with temperature can be substantially different. Two possible explanations for this difference are offered.

NASA TMX 54800  
Cat. 18

2004C  
504 MF

When Sample Only.

## INTRODUCTION

The standard ASTM method for determining tensile strengths of plastics by testing at a given temperature and at one selected strain rate is potentially inadequate for determining the tensile strengths of plastics when they are subjected to a broad range of strain rates and temperatures. In the temperature range above the glass transition temperature ( $T_g$ ) the time and temperature dependence of mechanical behavior of polymeric materials has been correlated by the WLF<sup>1</sup> equation and Smith's<sup>2</sup> failure envelope. However, no similar general concepts have been reported for correlating mechanical behavior of plastics in the temperature range below their  $T_g$ . Knowles and Dietz<sup>3</sup> showed that the yield stress of poly(methyl methacrylate), (PMMA), was strongly dependent on temperature and strain rate. Lohr and Parker<sup>4</sup> showed that the yield stress of PMMA determined at different temperatures and strain rates could be shifted laterally to construct a yield stress master curve which, in turn, could be approximated by a simple equation containing the applied strain rate,  $\dot{\epsilon}$ , and a temperature dependent shift factor,  $a_T$ . In the present study, the applicability of the yield stress master curve concept to PMMA over a greater temperature and strain rate range and to three additional plastics was investigated. In addition, the correlation between the temperature dependence of stress relaxation, yield stress and torsional damping was studied.

To test the generality of the yield stress master curve concept three additional materials were chosen which exhibit slightly different behavior from PMMA. Polystyrene (PS) has a high inherent flaw size,<sup>5</sup> polyvinyl chloride (PVC) generally behaves in a ductile manner during tensile tests

and polyethylene terephthalate (Mylar) is partially crystalline. Torsional damping, tensile-yield stress, and stress relaxation were measured for the four materials over the approximate temperature range of  $T_g + 15^\circ \text{C}$  to at least  $T_g - 100^\circ \text{C}$ . Yield stress master curves (yield stress versus strain rate times a temperature dependent constant) for each material were constructed and the constants for the equation<sup>4</sup> were calculated. The temperature dependence of the shift factors determined by construction of yield stress and stress relaxation curves was compared by somewhat arbitrarily referencing them to the temperature,  $T_r$ , where the logarithmic decrement of the amplitude of free torsional oscillations was equal to 0.5. This allowed direct comparison of the temperature-dependent behavior of the four materials.

## EXPERIMENTAL

### Materials

The four principal materials used were purchased as sheet stock from Cadillac Plastics Co. They will be referred to herein as follows:--Plexiglass G as PMMA-G, polystyrene as PS, polyvinyl chloride as PVC and polyethylene terephthalate as Mylar. The first three materials were nominally 1/32 inch thick and the Mylar was 0.010 inch thick. The commercial materials were used because of the large number of tensile specimens required for verification of the master curve concept. To allow limited comparison of the yield stress and torsional damping behavior of the PMMA-G with poly(methyl methacrylate) of known composition, several 10- by 10-inch sheets of poly(methyl methacrylate) referred to as PMMA-I were prepared at Ames. The PMMA-I was prepared by polymerization methods previously

described,<sup>6</sup> except in this instance the monomer and initiator were introduced into molds which had teflon gaskets between glass plates and which were evacuated and then purged with dry nitrogen. The molds were held at 60° C for 24 hours and then at 110° C for 48 hours. The resulting sheets were optically clear but the thickness of each sheet varied from approximately 0.025 to 0.035 inch; however, within a given specimen, the variation in thickness did not exceed 0.003 inch.

The materials were characterized mechanically by the freely oscillating torsional pendulum described previously.<sup>6</sup> The logarithmic decrement,  $\Delta$ , versus temperature curves for the five materials are shown in Fig. 1. This logarithmic decrement is defined as the natural logarithm of the ratio of the amplitudes of successive free oscillations. The data plotted show that the damping for each material peaks within a narrow range of temperatures; however, as indicated by the dashed lines, the peak temperature could not be directly determined in most of these tests. The approximate peak temperatures for the four commercial materials are indicated on the figure and given on table I. However, because of the uncertainty of the location of the peak of the damping curve, a point on the ascending portion of the curve was chosen as a reference temperature,  $T_r$ , for each material. The glass transition temperature,  $T_g$ , of the PMMA-I was previously<sup>6</sup> measured as 108° C. The damping curve has a value of  $\Delta = 0.5$  at 108° C for PMMA-I. Thus, the temperature at which  $\Delta = 0.5$  was defined as the  $T_r$  for each of the materials and is listed in column 2 of table I. These values of  $T_r$  should be approximately the glass transition temperatures of the remaining materials. However, it may be seen that  $T_r = 60^\circ$  C for PVC is approximately 15° to 16° lower than the accepted value<sup>7</sup> of  $T_g$  for this material. The

damping curve is also displaced a similar amount from that shown by Schmieder and Wolf.<sup>8</sup> Similarly, the value of  $T_r = 82^\circ \text{C}$  for PS is  $18^\circ \text{C}$  lower than the accepted value<sup>7</sup> of  $T_g$ , although data on polystyrene have been reported<sup>9</sup> with a  $T_g$  of  $82^\circ \text{C}$ . As will be shown in the discussion section of this paper, the values given in column 2 of table I probably are within  $\pm 2^\circ \text{C}$  of the glass transition temperatures of these two commercial materials and the differentials in  $T_g$  noted above may be attributed to additives in the sheet stock which act as plasticizers.

#### Test Equipment and Methods

The torsional damping curve was determined by the instrument and methods previously described,<sup>6</sup> except that in the transition region the temperature was increased in increments of  $5^\circ \text{F}$  instead of  $10^\circ \text{F}$  and then the sample was given 10 minutes for its temperature to equilibrate. Temperatures for all of the torsional damping, tensile-yield stress, and stress relaxation tests were measured with a potentiometer to  $\pm 1/2^\circ \text{C}$ .

The tensile tests for constructing master curves were run at constant strain rates in a Baldwin FGT 56 testing machine fitted with a Missimer furnace to control temperatures. For temperatures above ambient, the Missimer furnace was modified so that two coils supplied heat at a constant rate. Below ambient temperatures a variac powered Cal-Rod in a liquid nitrogen boiler supplied a constant flow of gaseous nitrogen. The control sensor was placed on the outlet side of the air circulation fan. Two heating coils then controlled temperatures both above and below ambient. These modifications produced  $\pm 1/2^\circ \text{C}$  controlled over the length of the test period. Some additional tensile tests were run in a Plas-Tech 591 high-speed tensile test

machine over a strain rate range of 0.007 to 300 in./in./min. These tests were made to verify the continuity of the increase in yield stress at higher strain rates than those available in the Baldwin machine. These tests in the Plastech machine were run at  $24^{\circ} \pm 2^{\circ}$  C. Standard ASTM D-638 tensile specimens were cut from single sheets of each of the four commercial materials for both the stress-relaxation and tensile tests. Because of the small amount of PMMA-I available and the variation in thickness across each sheet, smaller specimens with cross sections of 0.250 inch wide and over-all length of 3-1/2 inches were tested to compare the tensile strength of the PMMA-I and PMMA-G. The small specimens of PMMA-G were tested to determine if there was a specimen size effect. The strain rate was determined by dividing the crosshead speed by the distance between grip faces which was 3-1/2 inches for the D-638 specimens and 2-1/2 inches for the smaller specimens. That this procedure gave the true strain rate within  $\pm 3$  percent through the yield point was verified by comparison with rates determined by placing Baldwin Microformer extensometers directly on the gage section of the specimens.

The stress relaxation was measured with the instrument shown in Fig. 2. The specimen is elongated by a known and reproducible amount by an essentially instantaneous stroke of the linear actuator, and the load is thereafter recorded as a function of time. The instrument was designed for high stiffness, rapid loading and reproducible displacements. The plunger, which is linked to the wedges, could be activated either electrically or mechanically so that the entire loading process was completed in not over 0.04 second. Data were then taken starting at 0.4 second after the initial load application. The displacement, which was 0.050 inch for all tests reported here, was reproducible within  $\pm 0.0002$  inch as measured by SR-4 strain gages.

on a specimen and a linear variable differential transformer fastened to the two grips. The assembly in Fig. 2 was mounted on the front panel of a Statham SD-8 air bath temperature control cabinet. The Kulite Bytrex JP-100 semiconductor load cell was excited by a Harrison Lab 6226A power supply. The load cell output was recorded on a Texas Instruments Oscilloriter. The test sequence consisted in cooling the specimen to the lowest temperature for the particular series to be run, letting the temperature equilibrate for one hour, taking up slack to account for thermal expansion or contraction, loading, and allowing the specimen to relax for approximately 30 minutes, thus producing a relaxation curve extending over nearly 4 decades of time. The specimen was then unloaded and the next higher temperature set.

## RESULTS AND DISCUSSION

### Yield Stress Master Curves

Three definitions of yield stress are employed in this paper. Three distinct types of behavior were observed depending on the particular material and temperature. The first type is known as brittle behavior and is observed when a material suddenly fails while still in the ascending portion of its stress-strain curve. In this case, the yield stress is the failure load divided by the initial cross-sectional area. Thus, it is essentially equal to the true failure stress if the cross-sectional area has not decreased significantly. The second type is associated with the temperature range in which plastics behave in a manner similar to low carbon steel; that is, they show a definite yield with subsequent easily observable reduction in cross-sectional area and then proceed to fail. In this second case, the yield stress is calculated from the peak load at the first yield point and might

actually be significantly greater or less than the true failure stress. The third type for plastics seems to occur in the region of their glass transition temperature. Here the stress-strain curve is similar to that of aluminum in that the stress as a function of strain increases at a decreasing rate. However, for the region above  $T_g$  this stress-strain behavior in plastics can continue to strains of 100 percent or more. Here the yield stress has been calculated from the load at which a line drawn from 2-percent strain parallel to the initial slope of the load-strain curve intersects the curve. This load is then divided by the initial cross-sectional area. Each of the four materials discussed exhibit at least two of these three types of behavior in the temperature range covered.

Yield stresses of PMMA-G determined at the temperatures shown and at strain rates from approximately 0.005 to 3 in./in./min were shifted laterally to construct the master curve of yield stress,  $\sigma_y$  versus strain rate,  $\dot{\epsilon}$ , times the temperature shift factor,  $a_T$ , as shown in Fig. 3. The curve is referenced at  $T_r = 106^\circ$ ; thus  $a_T$  has the value of 1 at this temperature and Fig. 3 could be used directly to predict yield stresses at this temperature for the strain rates shown. More discussion about the values of  $a_T$  will be given later in this section. Yield stress master curves constructed in a similar manner are shown for Mylar, PS, and PVC in Figs. 4, 5, and 6, respectively. In general, the yield stresses in Figs. 3 through 6 vary approximately linearly with the logarithm of the strain rate. Thus, each master curve in the four figures has been approximated by a straight line. The data of Figs. 4, 5, and 6 fall very closely along one straight line, whereas the PMMA-G data in Fig. 3 might have been approximated by two lines. It is interesting to observe that for PMMA-G, the steeper slope which seems to occur in the curve for yield stresses determined



at 40° C and lower corresponds to the temperature range below the secondary damping peak observed in Fig. 1. The other three materials do not have this secondary damping peak and have a more linear relationship between yield stress and strain rate.

The straight lines drawn through the yield stress master curves may be represented by an equation of the form:

$$\sigma_y = K_1 + K_2 \ln \frac{\dot{\epsilon}}{\dot{\epsilon}_1} a_T \quad (1)$$

where  $\sigma_y$ ,  $\dot{\epsilon}$ , and  $a_T$  are as defined above;  $K_1$  and  $K_2$  are constants which depend on the type of material and on the reference temperature chosen; and  $\dot{\epsilon}_1$  is equal to 1 in./in./min. For this paper,  $\sigma_y$ ,  $K_1$ , and  $K_2$  will be in units of psi,  $\dot{\epsilon}$  in units of in./in./min, and  $a_T$  is dimensionless. This is the same general equation reported previously<sup>4</sup> except that the constants have been recast to allow easier calculation of yield stress from a given strain rate and shift factor. The values of the constants  $K_1$  and  $K_2$  and the stress and temperature limits of applicability of equation (1) as determined in this series of tests are given in table I.

Equation (1) could be used to determine yield stresses at any temperature within the range studied and over a wide range of strain rates, including those not readily available in the laboratory. Yield stresses calculated from equation (1), the constants of table I, and the shift factors,  $a_T$ , derived from the construction of the master curves, were compared with yield stresses determined from tensile tests run on a Plas-Tech 591 tensile test machine. The comparison is shown in Fig. 7 where yield stresses are plotted as a function of strain rate. The agreement is very satisfactory.

The yield stress master curves for the small samples of PMMA-G and PMMA-I are compared in Fig. 8. Also in Fig. 8 is the straight line approximation of the master curve for the larger samples of PMMA-G used to obtain the data of Fig. 3. It may be seen from Fig. 8 that the master curves of PMMA-G and PMMA-I were essentially the same within the scatter of the data. The straight line approximation from Fig. 3 also fits the data of Fig. 8 quite well, indicating that the effect of specimen size is small.

#### Relations Between $a_T$ Shift Factors

Just as it was possible to gain insight into polymer behavior in the temperature region above the glass transition temperature,  $T_g$ , by use of the WLF equation,<sup>1</sup> it should be possible to learn something about the behavior of polymers at temperatures below  $T_g$  by comparing the  $a_T$  shift factors determined by construction of yield stress and stress relaxation master curves. To this end, Figs. 9 through 12 contain the shift factors  $a_T$  plotted as a function of temperature for the four principal materials. Shift factors used for constructing both the yield stress and stress relaxation master curves are shown for each material. In all cases,  $a_T$  has the value 1 at the reference temperature. Where possible, data from other authors have been compared with the experimental shift factors determined as part of this work. To include the shift factors of these authors properly, it was necessary to know what reference temperature to use. Tobolsky et al.<sup>10</sup> define a reference temperature,  $T_1$ , as the temperature at which the relaxation modulus attains the value of  $10^9$  dynes/cm<sup>2</sup> in 10 seconds. The relaxation modulus is defined as the time-dependent stress

divided by the imposed strain. Values of  $T_i$  derived with Tobolsky's definition were calculated from the current stress relaxation tests and included in table I as  $T_i'$ . This definition is not applicable to Mylar, however, because even at the highest temperature tested,  $130^\circ\text{C}$ , the modulus had not decreased to  $10^9$  dynes/cm<sup>2</sup>. It may be seen from table I that  $T_i'$  and  $T_r$  are close enough to be used interchangeably. Thus, it should be possible to compare other investigators' work, which is referenced at  $T_i$ , with the current data which are referenced at  $T_r$ . It will be necessary only to shift their data laterally an amount equal to  $T_i - T_r$ .

Therefore, in Fig. 9, where the data of Tobolsky et al.<sup>11</sup> and Iwayanagi<sup>12</sup> have been included, the data of ref. 11 ( $T_i = 109^\circ\text{C}$ ) have been shifted  $3^\circ\text{C}$  to the left, and the data of ref. 12, which have a  $T_i$  of  $119^\circ\text{C}$ <sup>11</sup> were shifted  $13^\circ\text{C}$  to the left. The data for polystyrene<sup>11</sup> shown in Fig. 11 were shifted  $21^\circ\text{C}$  left. Ward's<sup>13</sup> data on Mylar (fig. 10) did not include a reference temperature; therefore, the  $a_T$  shift factors were arbitrarily plotted so that  $a_T = 1$  at  $T_r = 96^\circ\text{C}$ .

In both Figs. 9 and 11 the agreement among the stress relaxation shift factors (SR  $a_T$ ) determined in this study and those from refs. 11 and 12 is seen to be quite good indicating the correctness of the temperature referencing system just described. The divergence of SR  $a_T$  in the  $65^\circ$  to  $80^\circ\text{C}$  temperature region shown in Fig. 10 may be due to improper referencing or could easily be due to differences in crystallinity as Ward's material was in mono-filament form.

A general observation which may be made from studying Figs. 9 through 12 separately is that, in general, the yield stress shift factor (YS  $a_T$ )

points lay below the SR  $a_T$  points in the region below  $T_g$ . Two possible explanations for this may be given. In the vicinity of the glass transition temperature,  $T_g$ , and above, the temperature dependence of SR  $a_T$  and YS  $a_T$  (or failure stress  $a_T$ ) is given by the WLF equation<sup>2</sup> and is the same for both. However, beneath  $T_g$ , as the strain increases, the relation between stress and strain may become nonlinear (i.e., at the same increment of time after loading, twice the imposed strain will not produce twice the stress). This nonlinearity would cause lower yield stresses and consequently lower incremental YS  $a_T$ . This argument is consistent with the experiments because the SR  $a_T$  were determined at 1.43 percent strain, whereas the YS  $a_T$  were determined at generally higher strains up to about 4 percent. The other possible explanation is that the material is not able to reach its "true yield stress" before it fails, because cracks propagate from inherent flaws as discussed by Berry.<sup>5</sup> This true yield stress would be the yield stress which might be calculated from a strength theory such as Bueche's<sup>14</sup> which is formulated for materials in their glassy state or from equation (1) using SR  $a_T$ . Although these two general effects will be additive, it is felt that the latter probably explains the major portion of the wide diversity between SR  $a_T$  and YS  $a_T$  for PS shown in Fig. 11. The difference in slope of the two sets of points then would indicate an increasing inherent flaw size with decreasing temperature. Close examination of Berry's<sup>5</sup> work indicates that the inherent flaw size increases with increasing strain rate. The proposed mechanism is therefore consistent with Berry's work because of the demonstrated equivalence between decreasing temperature and increasing strain rate.

The  $YS a_T$  for all four materials are shown in Fig. 13. Here the  $YS a_T$  points in Figs. 9 through 12 have been plotted so as to pass through a common reference temperature. Thus, the figure consists of shift factors plotted against the difference between the test temperature and the reference temperature. The strong similarity in the temperature dependence of  $YS a_T$  for PMMA-G, PVC and Mylar may easily be seen. It is also not surprising, in light of the just discussed temperature-dependent flaw mechanism, to see that for PS the  $YS a_T$  fall below those for the other three materials.

The best fit curve for PMMA-G, Mylar and PVC of Fig. 13 is carried over into Fig. 14 where  $SR a_T$  are plotted against the difference between the test temperature and the reference temperatures of each material. Here the agreement among the four materials is not as good as for the  $YS a_T$  shown in Fig. 13. However, in both figures there are some definite differences. For instance, in the transition or reference temperature region, the slope of the  $a_T$  points for PVC is definitely greater and that of Mylar less than the average slope of the PMMA-G and PS  $a_T$  curves. Also, the incremental  $SR a_T$  cannot be measured as accurately as the  $YS a_T$  because the percent change in the stress relaxation modulus in the glassy state is often much less than the change in yield stress. This would accentuate errors in reproducibility of the displacement distance in the stress relaxation system shown in Fig. 2. Attaining reproducibility at temperatures between freezing and cryogenic temperatures is made difficult by some stickiness of the loading mechanism and frost buildup on the wedges.

It should be pointed out that, at least at this stage of the development of polymer science, it should not be expected that the shapes of the  $a_T$

versus temperature curves in the glassy region would superpose in a manner similar to that described by the WLF equation above  $T_g$ . Current theories<sup>15</sup> hold that relaxation below  $T_g$  consists of side group motions; thus different materials, because they have different side groups, would not be expected to relax at the same rate or have the same temperature dependence. The relations noted in this paper are therefore primarily of phenomenological interest but may also be of use in understanding basic polymer behavior.

#### CONCLUDING REMARKS

The concept of the yield stress master curve was applied to the four materials studied, poly(methyl methacrylate), polyvinyl chloride, polystyrene, and polyethalene terephthalate, and seems to be an effective way of correlating the temperature and strain rate dependence of their yield stresses even though the master curves may cover a behavior range encompassing brittle, brittle-ductile, and highly ductile behavior. These master curves can then be described by a simple equation involving two constants, one of which depends on the nature of the material and the other on the reference temperature chosen. The equation is applicable over a range of yield stresses of approximately 1,000 to 20,000 psi with two exceptions. One exception is for PS, because the yield stresses do not go above about 8,000 psi; the other exception is for Mylar below 4,000 psi because crystallinity apparently causes the yield stresses to be higher than given by the equation. The approximate temperature range for application of the equation is from  $T_g$  to at least 100° C below  $T_g$ .

Comparison of the shift factors required for constructing both yield stress and stress relaxation master curves showed a strong similarity in

the temperature dependence of the four materials. However, the temperature dependence does not appear to be identical for all materials, nor is it the same for both yield stress and stress relaxation, as it is above the glass transition temperature. The slightly lower yield stress shift factor curve of PVC and PMMA-G is thought to be a manifestation of nonlinearity at high loads, whereas the greatly divergent behavior of the PS shift factors is thought to be primarily due to failure initiated by temperature and strain rate dependent inherent flaws.

The reference temperature  $T_r$  picked from the torsional damping curve at  $\Delta = 0.5$  for each material seems to be approximately equal to  $T_i$  and  $T_g$  and can be used as a reference temperature in comparing behavior of different materials.

## REFERENCES

1. Williams, M. L., R. F. Landel and J. D. Ferry, J. Amer. Chem. Soc., 77, 3701 (1955).
2. Smith, T. L., ASTM Special Technical Publication No. 325 (1962).
3. Knowles, J. K. and A. G. N. Dietz, Trans. A.S.M.E. 77, 177 (1955).
4. Lohr, J. J. and J. A. Parker, Polymer Preprints, New York A.C.S. Meeting, 368 (1963).
5. Berry, J. P., J. Poly. Sci., L, 313 (1961).
6. Dudek, T. J. and J. J. Lohr, to be published in J. Appl. Poly. Sci.
7. Ferry, J. D., Viscoelastic Properties of Polymers, Wiley, New York (1961).
8. Schmeider, K. and K. Wolf, Kolloid - Z., 127, 65 (1952).
9. Jenckel, E. and R. Heusch, Kolloid - Z., 130, 89 (1953).
10. Tobolsky, A. V., D. Carlson and N. Indictor, J. Appl. Poly. Sci., 7, 393 (1963).
11. Takahashi, M., M. C. Shen, R. B. Taylor and A. V. Tobolsky, J. Appl. Poly. Sci., 8, 1549 (1964).
12. Iwayanagi, S., J. Sci. Res. Inst. Japan, 49, 4 (1955).
13. Ward, I. M., Polymer, 5, 59 (1964).
14. Bueche, F., Physical Properties of Polymers, Interscience: New York (1962).
15. Boyer, R. F., Rubber Reviews, XXXVI, 1303 (1963).



TABLE I.

Characteristic Parameters for the Materials Studied and the  
Limits of Applicability of Equation (1)

Material	$T_{\text{peak}},$ °C	$T_r,$ °C	$T_1',$ °C	$K_1,^*$ psi	$K_2,^*$ psi	Yield stress range, psi	Temperature range, °C
PMMA-G	126	106	106	2000	486	$1,000 < \sigma_y < 20,000$	-50 to 110
Mylar	110	96	N.A.	5840	405	$4,000 < \sigma_y < 22,000$	-37 to 110
PS	95	82	81	2160	358	$1,000 < \sigma_y < 8,000$	-16 to 90
PVC	70	60	61	3100	531	$500 < \sigma_y < 20,000$	-37 to 60
PMMA-I		108					

\* From  $\sigma_y = K_1 + K_2 \ln \frac{\dot{\epsilon}}{\dot{\epsilon}_1} a_T$

## List of Figures

- Fig. 1.- Torsional pendulum results for PMMA-G, PMMA-I, Mylar, PVC, and PS.
- Fig. 2.- Schematic diagram of stress relaxation instrument.
- Fig. 3.- Yield stress master curve for PMMA-G.
- Fig. 4.- Yield stress master curve for Mylar.
- Fig. 5.- Yield stress master curve for PS.
- Fig. 6.- Yield stress master curve for PVC.
- Fig. 7.- Comparison of results of tensile tests at  $24^{\circ} \pm 2^{\circ}$  C using Plas-Tech 591 with predictions of equation (1) using constants of table I obtained by use of Baldwin machine.
- Fig. 8.- Yield stress master curves for small specimens of PMMA-G and PMMA-I.
- Fig. 9.- Yield stress and stress relaxation shift factors for PMMA-G.
- Fig. 10.- Yield stress and stress relaxation shift factors for Mylar.
- Fig. 11.- Yield stress and stress relaxation shift factors for PS.
- Fig. 12.- Yield stress and stress relaxation shift factors for PVC.
- Fig. 13.- Comparison of yield stress shift factors with the temperature difference between test temperature and reference temperature for the four principal materials.
- Fig. 14.- Comparison of stress relaxation shift factors with the temperature difference between test temperature and reference temperature for the four principal materials.

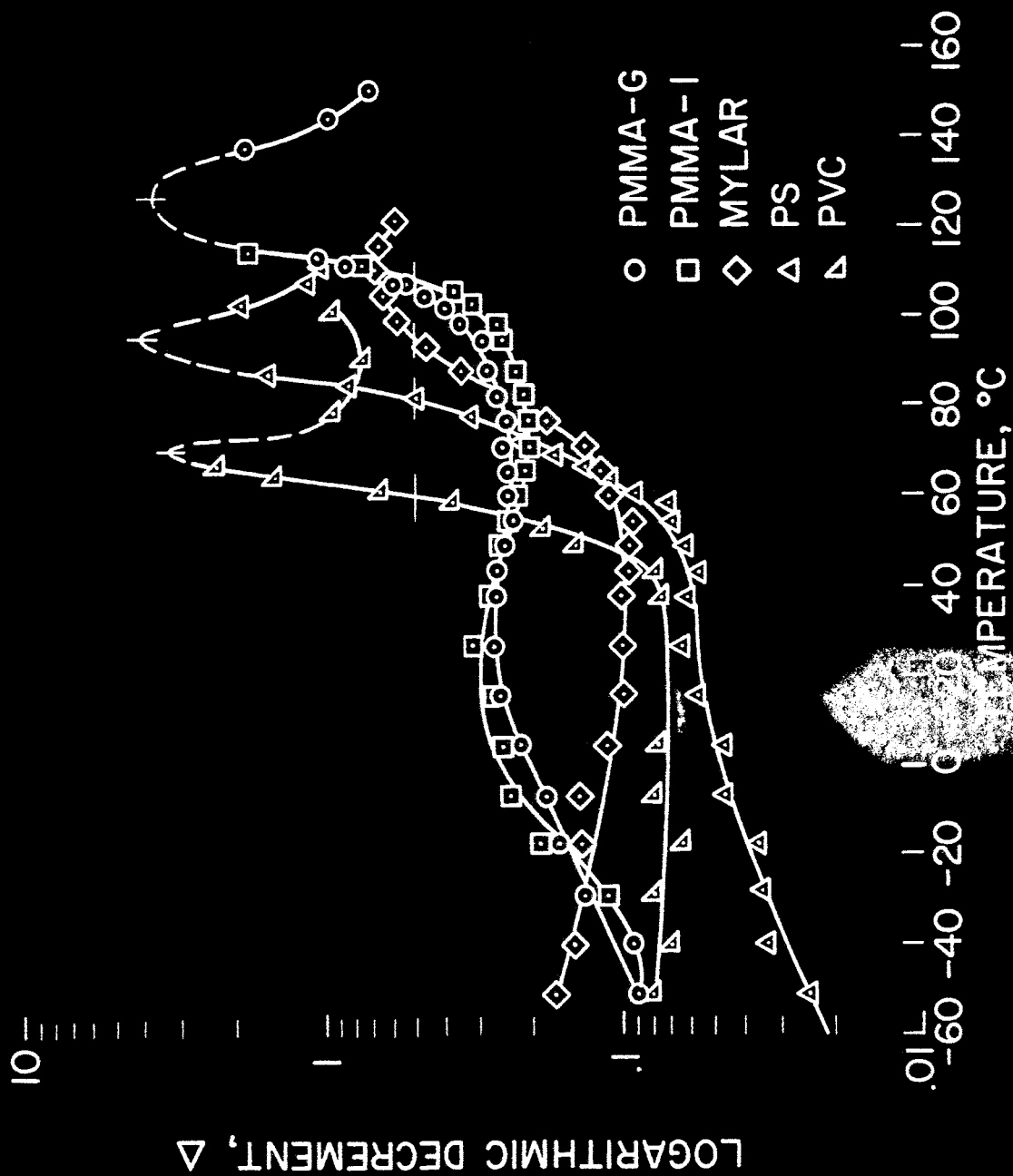


Figure 1.- Torsional pendulum results for PMMA-G, PMMA-I, Mylar, PVC, and PS.

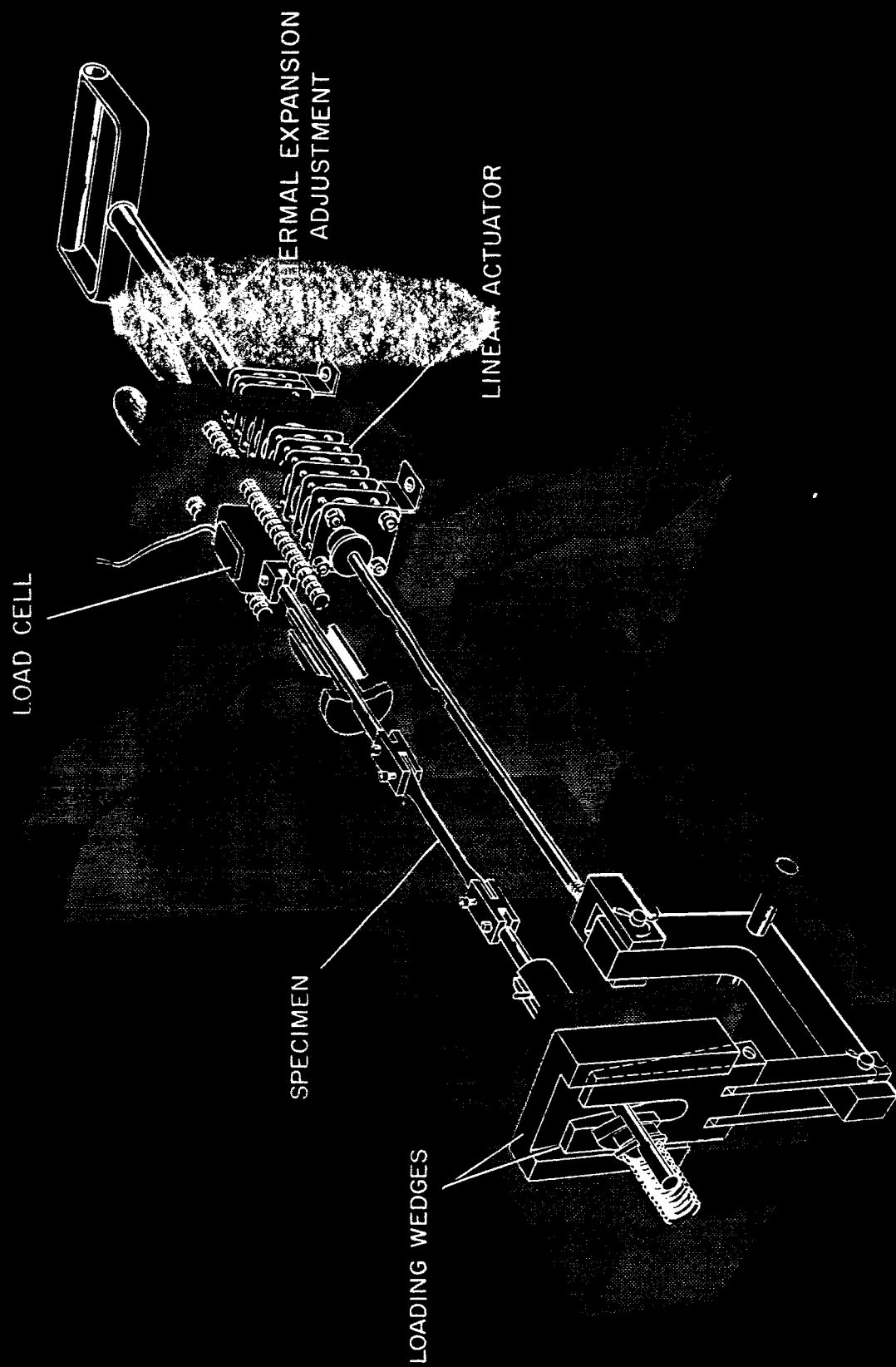


Figure 2.- Schematic diagram of stress relaxation instrument.

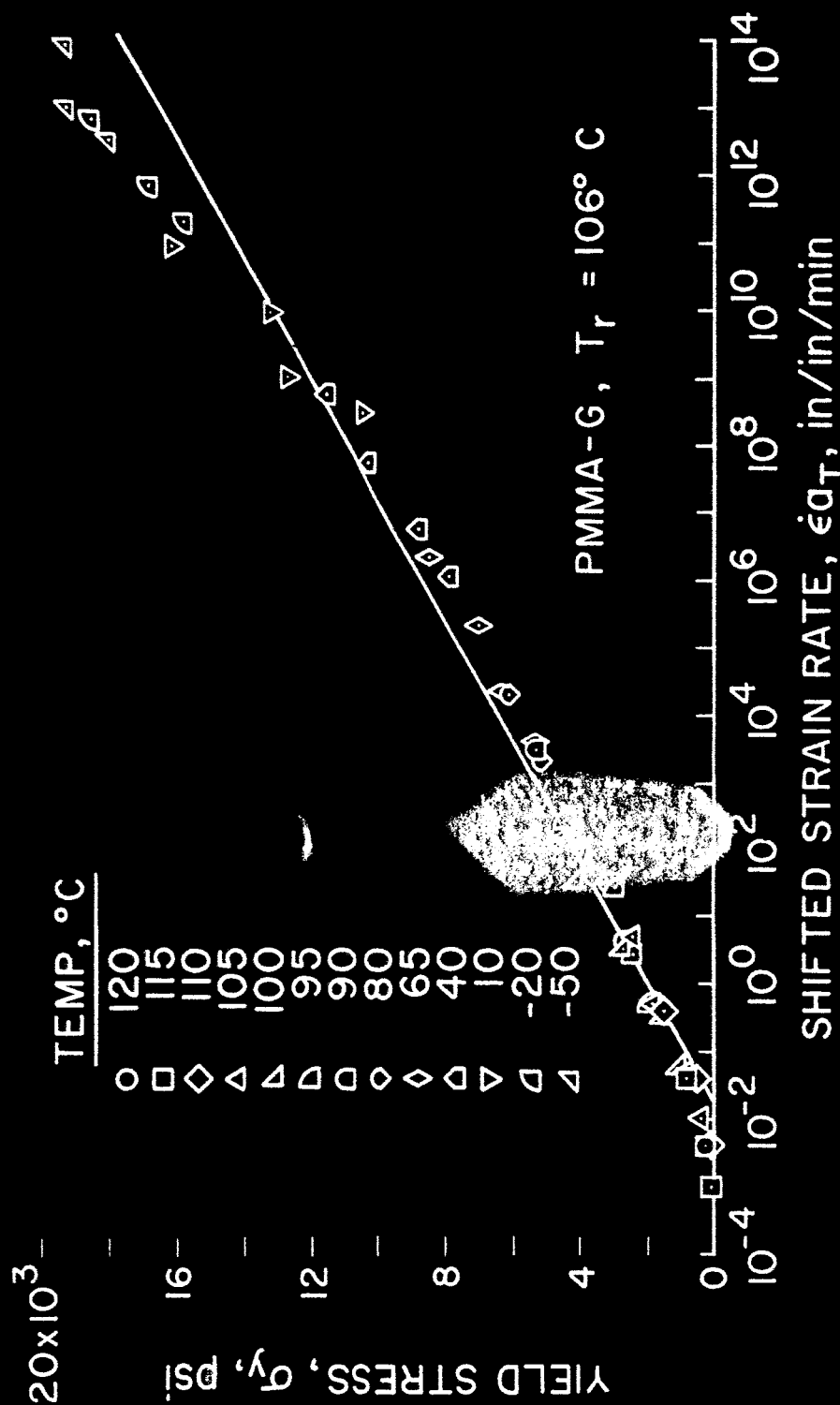


Figure 3. Yield stress master curve for PMMA-G.

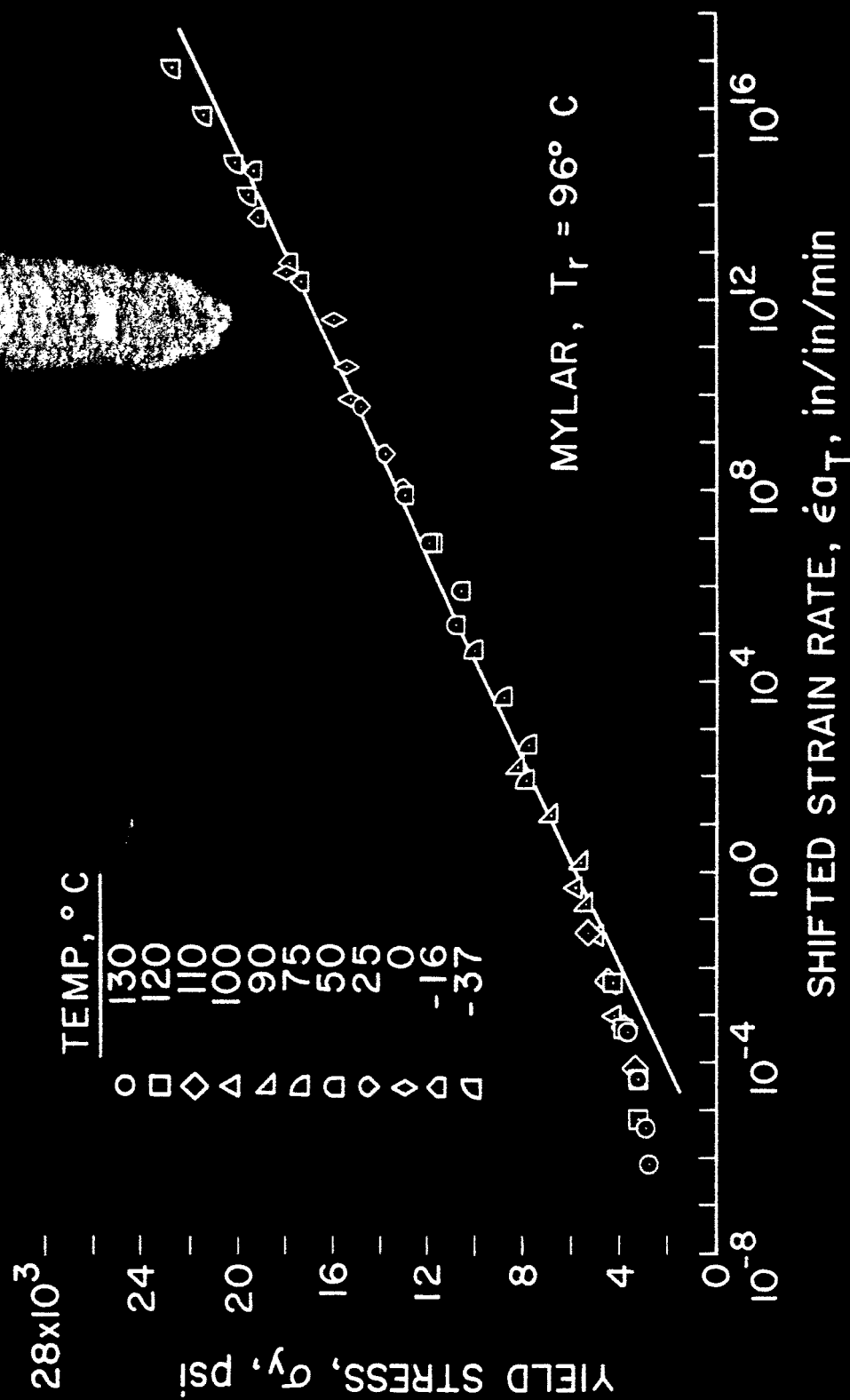


Figure 4. Yield stress master curve for Mylar.

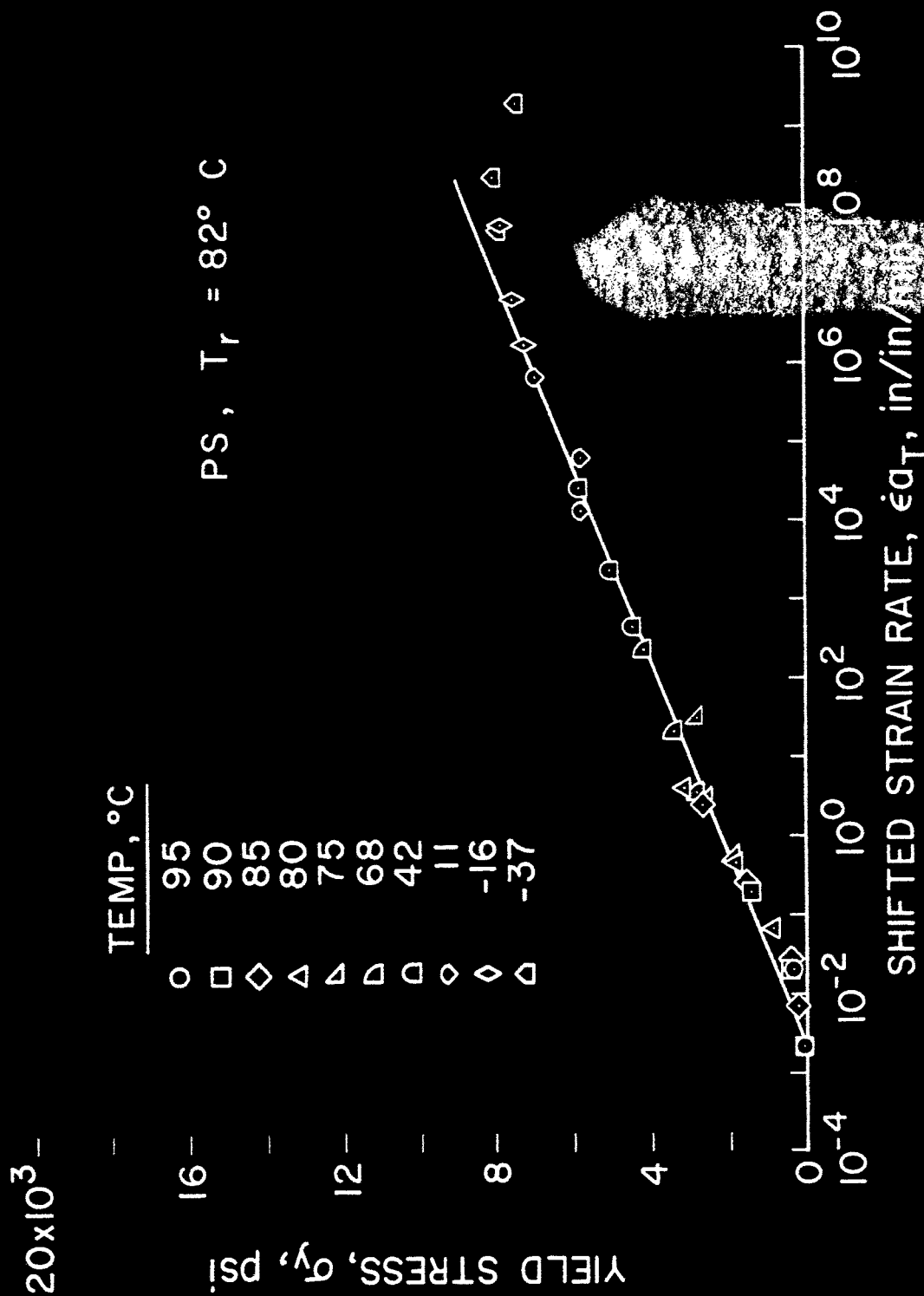


Figure 9.— Yield stress master curve for PS.

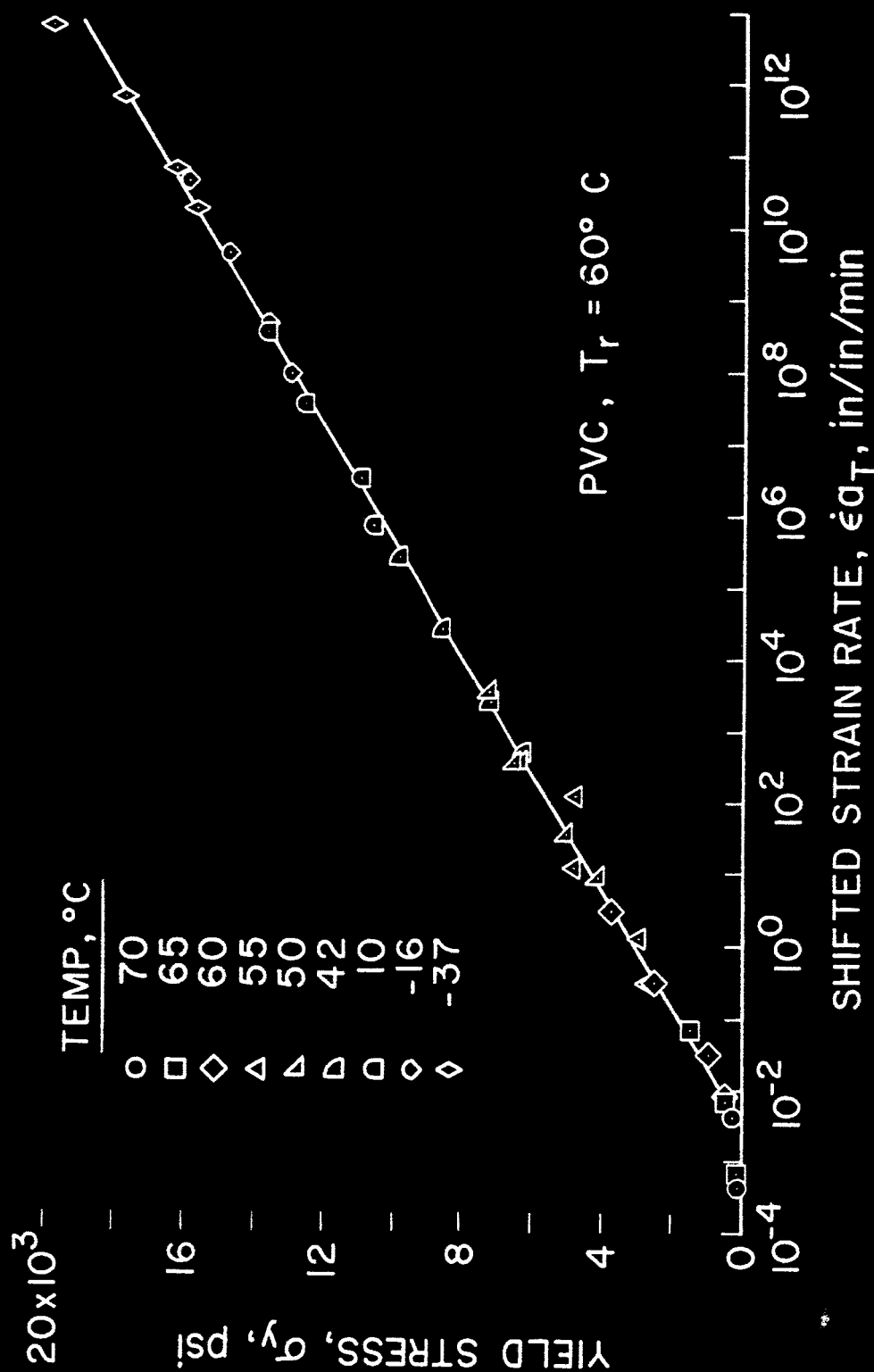


Figure 6-4 Yield stress master curve for PVC.



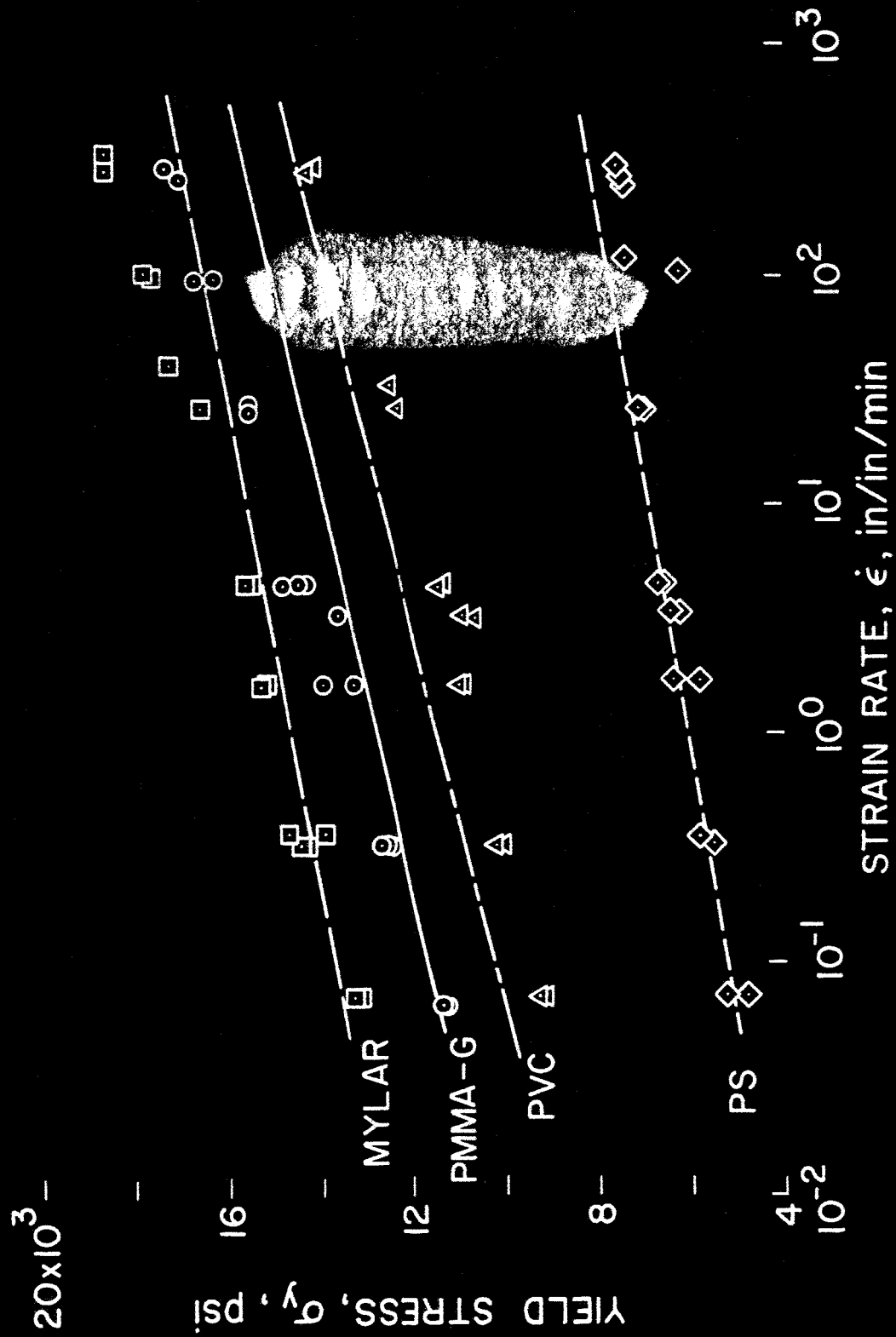


Figure 7.- Comparison of results of tensile tests at 24 420 C using Plan-Tech 591 with predictions of equation 1 using constants of Table 1 obtained by use of Baldwin machine.

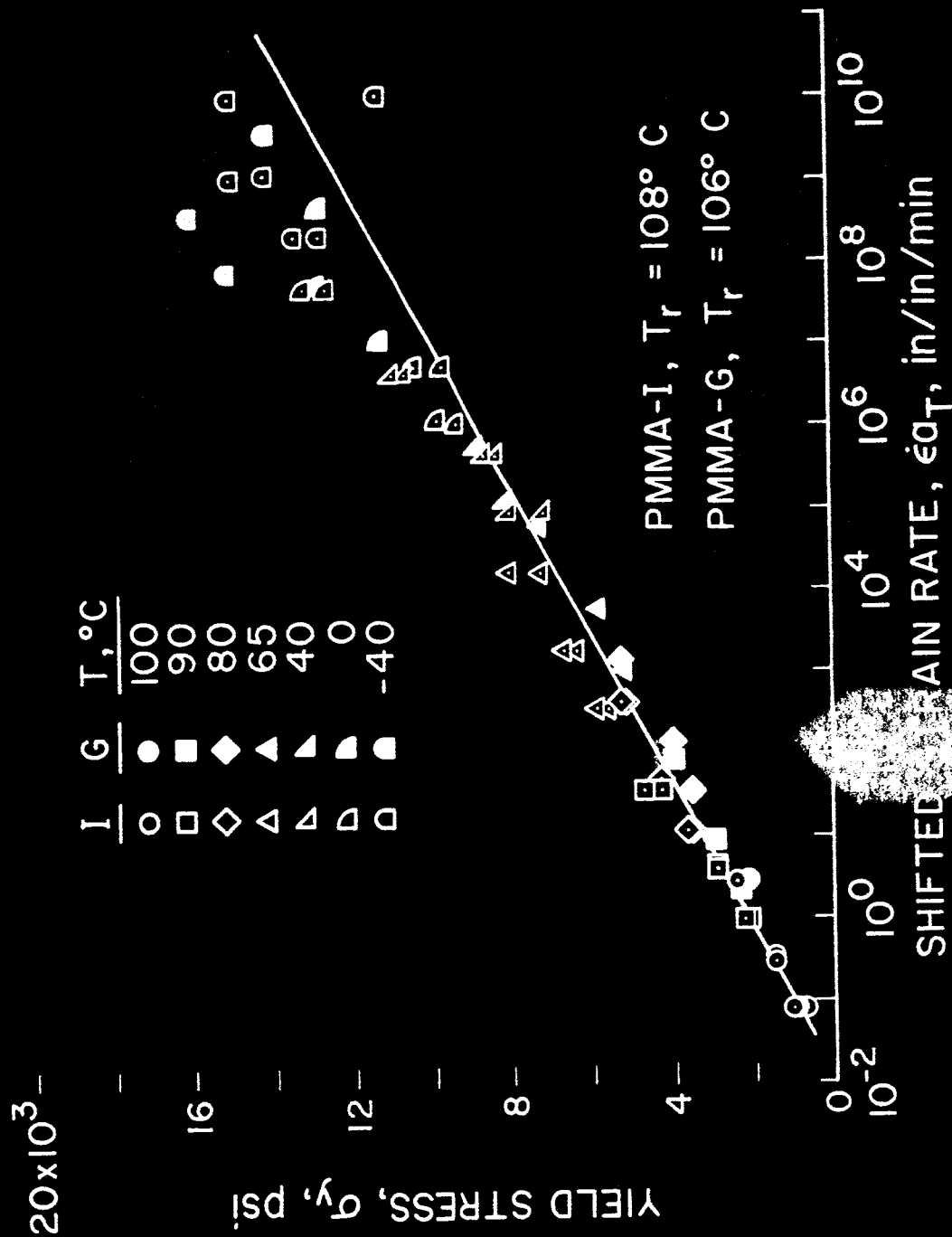


Figure 6.- Yield stress master curves for small specimens of PMMA-G and PMMA-I.

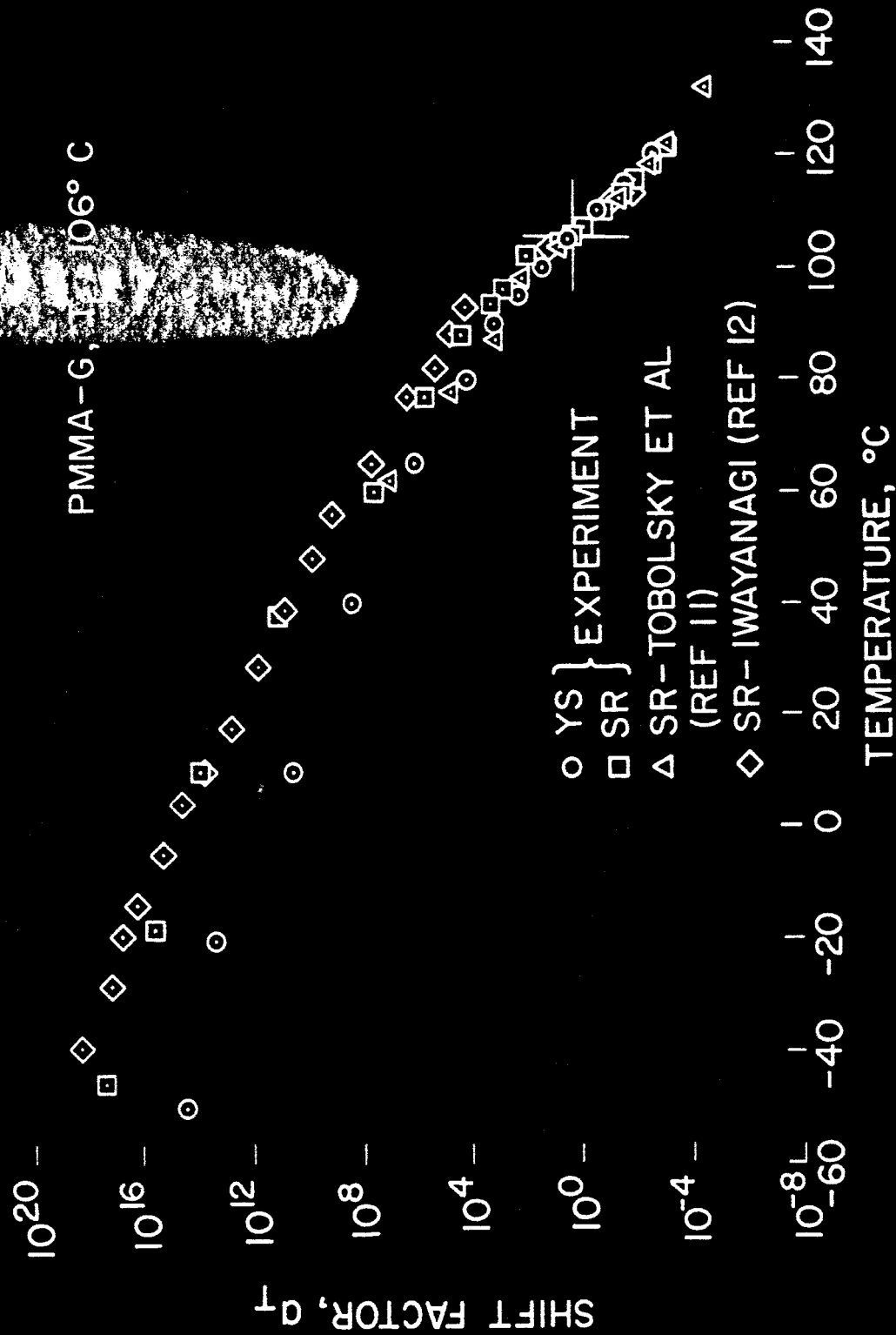


Figure 9. Yield stress and stress relaxation shift factors for PMMA-G.

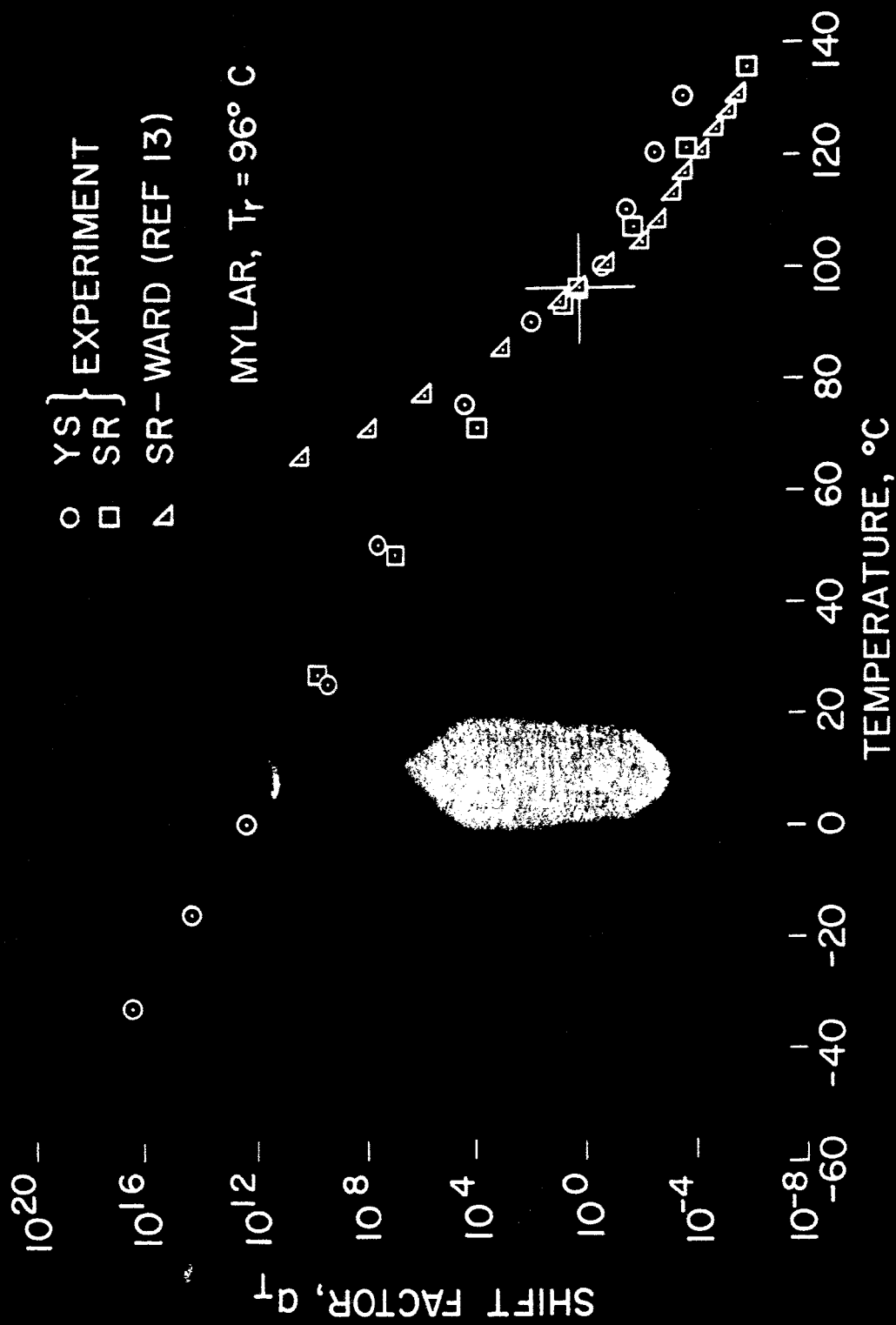


Figure 10. - Yield stress and stress relaxation shift factors for Mylar.

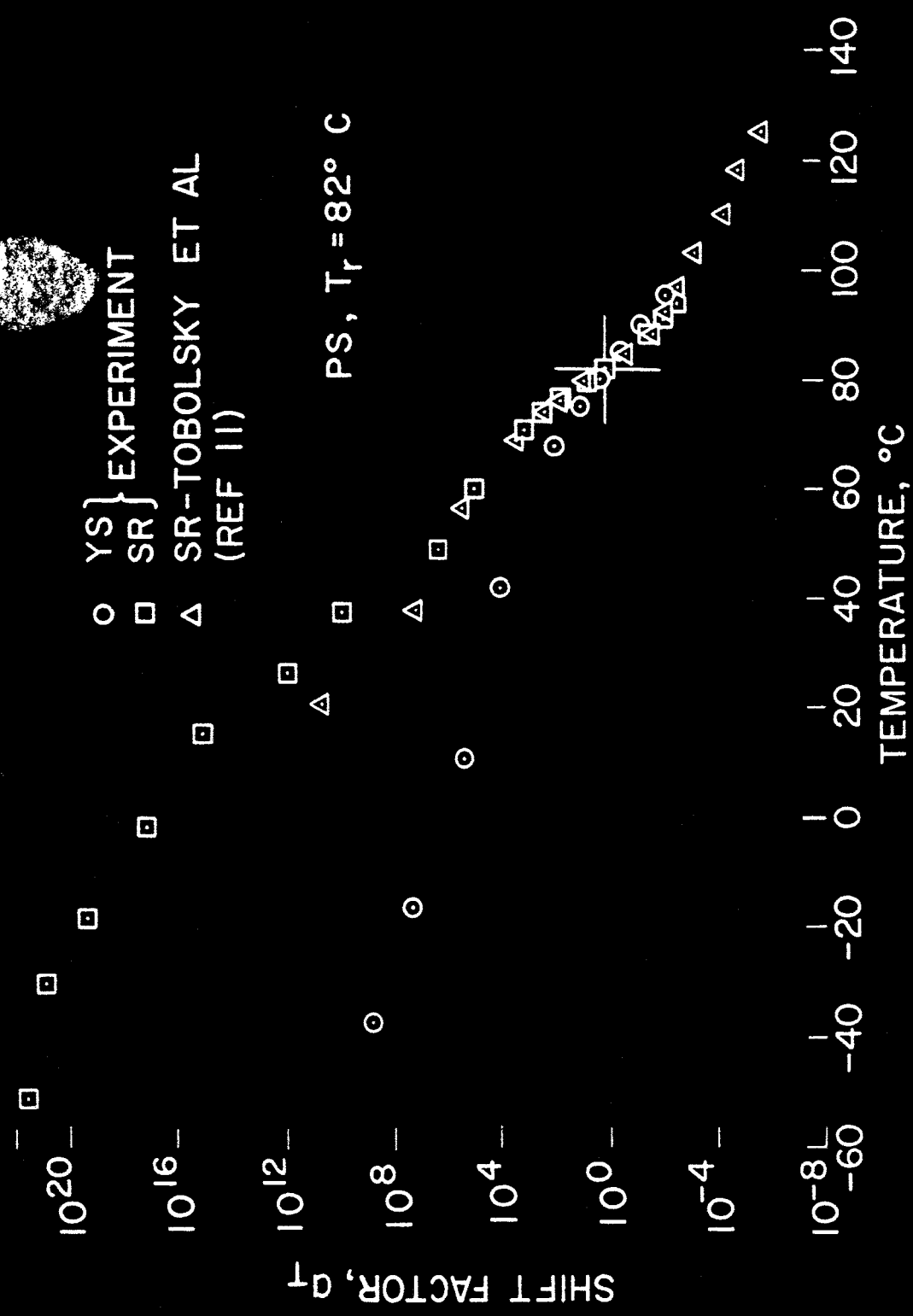


Figure 11. Yield stress and stress relaxation shift factors for PS.

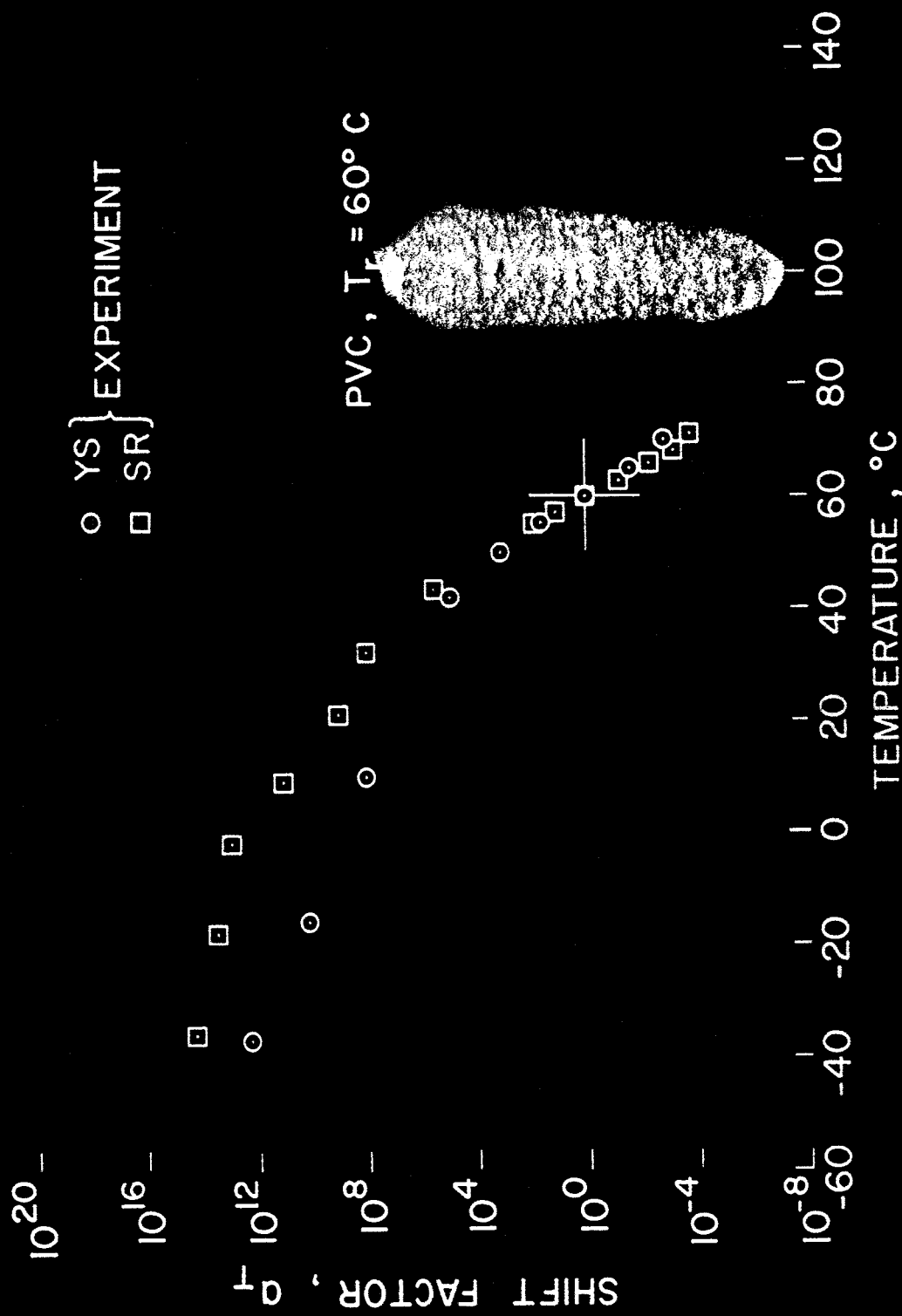


Figure 10. Yield stress and strain rate dependence of the shift factor for PVC.

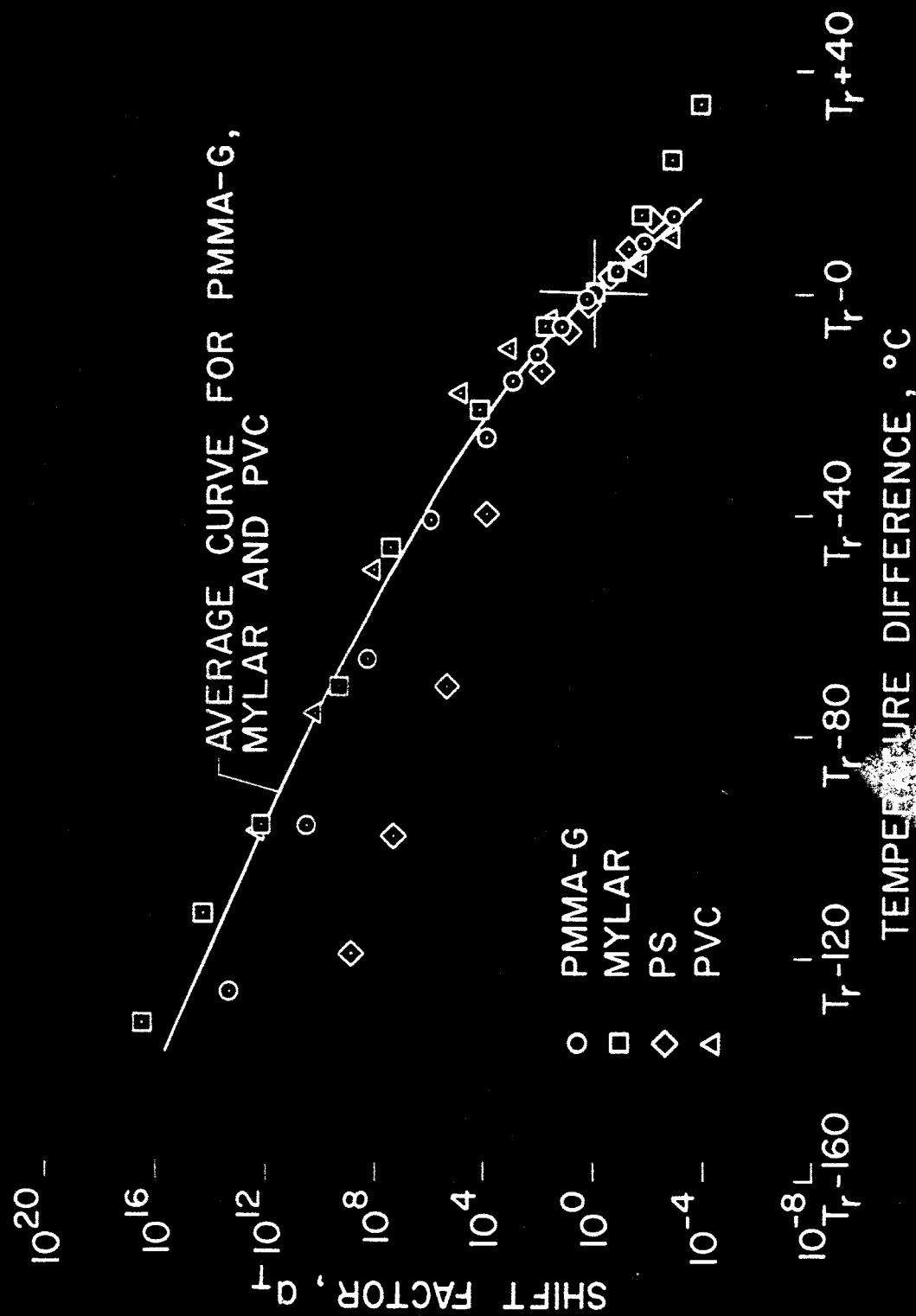


Figure 15. Comparison of yield strength with the temperature difference between test temperature and reference temperature for the four principal materials.

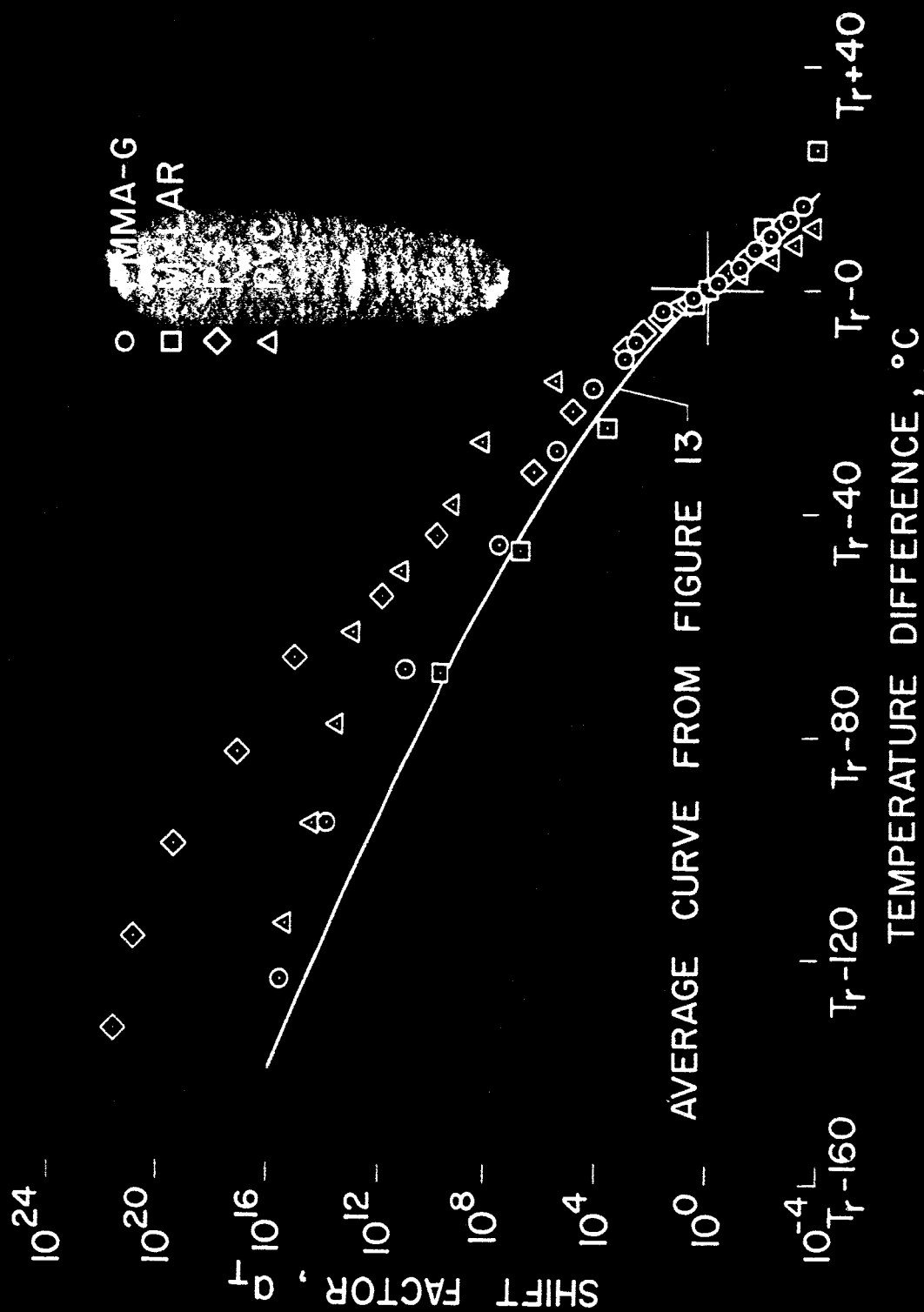


Figure 14.- Comparison of stress relaxation shift factors with the temperature difference between test temperature and reference temperature for the four principal materials.